Thermal Alteration and Differential Sublimation Can Create 3200 Phaethon's "Rock Comet" Activity and Blue Color

C.M. Lisse[a] and J. Steckloff[b,c] [a]JHU Applied Physics Laboratory [b]Planetary Science Institute [c]University of Texas at Austin e-mail: carey.lisse@jhuapl.edu

Introduction. Asteroid 3200 Phaethon is a small (~6 km diameter) asteroid that comes extremely close to the Sun (0.16 au, or more than twice as close as Mercury) every 1.4 years. At the same time, it is also one of the bluest asteroids known (there are only ~20 blue asteroids known versus ~200,000 red/grey ones) and is the source of the Geminid meteor stream the Earth intersects with each December. In [1] it was showed how these are all connected, in that the ~1100K noontime temperatures achieved at perihelion wander across its surface, boiling off any dark red refractory organics, red nanophase (microcrystalline) iron, and darkish pyroxenes, leaving behind relatively bright bluish surface material while creating “rock comet” activity, with gas production rate $Q_{gas} \sim 10^{22}$ molecules/sec that can help supply the yearly Geminids. The same mechanism should make any initially C-type body very blue and active, and indeed the nuclei of comets 96P/Machholz and 322P/SOHO are also anomalously blue and highly active. These predictions are testable by searching for signs of spectral bluening of the surfaces of other small bodies in Phaethon-like small perihelion orbits, and by *in situ* measurements of Phaethon's surface and coma composition near perihelion with the upcoming DESTINY+ mission [2,3] to Phaethon by JAXA.

Provenance. 3200 Phaethon (1983 TB), is an active Apollo asteroid [4-8] and parent body of the Geminids meteor shower of mid-December. It is on an 1.434 yr period, highly eccentric (e = 0.88990) orbit that brings it within 0.14 AU of the Sun, closer than any other named asteroid [9]. Identified in the 1983 IRAS sky survey [10-11] as the first asteroid ever discovered from space and classified as a rare B-subtype of the C-type asteroids [12-13], it has now been well characterized over 25+ orbits and is known to be an object ~6 km in diameter, rotating at about 3.6 hrs’ period, with a highly unusual blue color vs. other asteroids [4-5, 14].

Phaethon’s mass shedding and activity. A thermal driving mechanism for its mass loss into the Geminid stream has been proposed and studied by numerous recent authors [6-7, 9, 15-22]. [22] states an estimated minimum total mass for the Geminid meteoroid stream of 1.6×10^{16} g, while JPL Horizons 2019 quotes an estimated mass for Phaethon itself of 1.4×10^{17} g, only 8.75 times larger. By contrast, the mass required to optically resurface Phaethon out to 5 um would be only about 10 um (depth) * 3 g cm^{-3} (density) * 4p $R_{Phaethon}^2$ (surface area) ~ 5×10^9 g, about one millionth of the mass shed into the Geminid stream.

Spectroscopy: Composition & Color. Phaethon’s surface composition is by all accounts of carbonaceous chondrite material that has been heavily thermally altered. Its surface spectrum is *extremely* and unusually blue [24 -

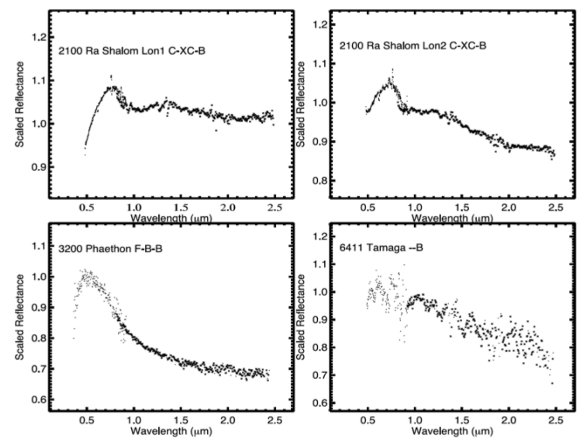

Figure 1: - ***(Left)*** Reflectance spectrum comparison for seven B-type asteroids, showing how extraordinarily **blue** Phaethon is with its 30% increase in relative reflectivity going from 2.5 down to 0.5 um, after [23]. (Typical asteroid color trends are **red** and run 5-10% amplitude over this wavelength range.)

26], increasing ~30% in reflectivity from 1.0 um down to 0.5 um (Fig. 1); in fact it is one of the bluest asteroids known. [24] found the best meteorite spectral matches for Phaethon’s spectrum to be Yamato-86720, an unusual CI/CM meteorite that likely has been heated up to 500–600 °C [27], and heat-treated Ivuna [28], while [23] found the best spectral matches to be the thermally processed CK4 meteorites ALH85002 and EET 92002. The CK4 meteorites are known for their highly oxidized, CAI, olivine, refractory metal sulfide, FeO_x plus highly refractory inorganic amorphous carbon/graphite matrix dominated composition due to extensive hot aqueous reworking of primitive ferromagnesian silicates, sulfides, and complex organics. Thus it is very plausible that the heating Phaethon endures during its perihelion passage has led to compositional alteration of its sensible surface.

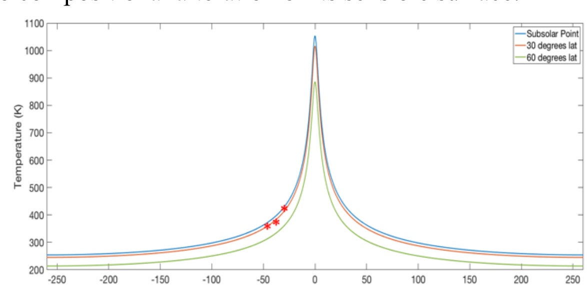

Figure 2: Phaethon surface temperatures at the sub solar point and at 30 and 60 degrees of latitude and the sub-solar longitude for the solid species shown in Fig. 1. The hottest points on Phaethon, near local Noon, climb above 1000 K for a few days near perihelion every orbit. Red Stars : 30 deg latitude model temperature estimates from rotationally resolved near-infrared spectroscopy of Phaethon’s surface by [29].

Thermophysical Analysis. We compute the temperatures across Phaethon's surface using the Many Materials Orbital Sublimation model (MaMOS; [30-33]), which employs conservation of energy, Clausius-Clapeyron, and Knudsen-Langmuir [34] relations to compute the surface temperature that balances solar energy with sublimative and radiative heat loss over a spherical surface. The resulting MaMOS Phaethon surface temperatures (Fig. 2) are consistent with recent thermophysical models of the surface [5, 9, 20, 35] that have the maximum dayside temperature reaching upwards of 1100 K for a Phaethon with Bond Albedo = 0.043, Emissivity ~ 0.9, and beaming parameter = 0.9, despite its relatively quick rotation rate of 3.6 hrs and high thermal inertia of ~600 +/- 200 J m^{-2} K^{-1} $s^{-1/2}$. The MaMOS temperature also appear consistent with thermal modeling of Phaethon constrained by observations ([29]; Fig. 2).

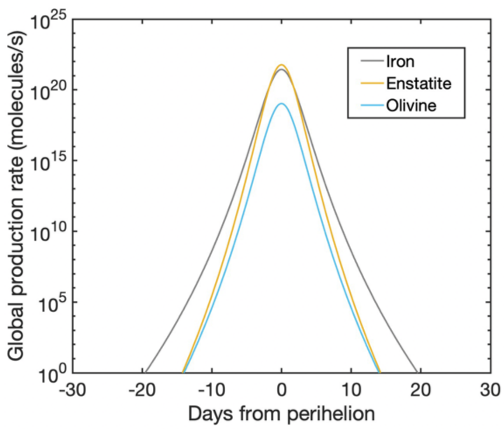

Figure 3: Predicted total body outgassing rate vs heliocentric distance for a 2.9 km radius spherical Phaethon using the MaMOS model [30, 32, 36].

Sublimation Behavior. Using the model curves of [36-37], surface temperature profiles translate into local saturation vapor pressures for exposed surface solid species that are highly non-linear in the local surface temperature. Integrating across the surface to compute the maximum total sublimative molecular production from Phaethon at each point along its orbit (Fig. 3) and find that Phaethon can lose up to ~10^{22} molecules/s of iron (depending on the $P_{sat}(T)$ literature model used) at perihelion. I.e., for a $T_{surface\ max}$ = 1080 K model at the sub-solar point (i.e., local noon) at perihelion, we find that the 5.2 x 10^{11} cm^2 of Phaethon's surface loses about 9 monolayers of Fe on average each day; it takes only about 2.7 hours to remove an entire monolayer, and about 50 monolayers are removed in each orbit. One micron's worth of Fe is removed in only 1000 years, much faster than the estimated ~1 Myr timescale to redden the same surface via space weathering [38-43]. Thus the optical characteristics of the surface can be changed via thermally driven sublimation. The same arguments just given are also applicable to Mg-rich pyroxene endmember enstatite, which has similar sublimative temperature dependence to Fe at 500 – 1100K (Fig. 2), yielding a sublimative mass loss rate of pyroxene at the ~10^{22} mol/sec level (depending on the $P_{sat}(T)$ literature model used) at perihelion (Fig. 4). The sublimative loss of bulk enstatite materials can thus weaken the surface solid matrix of Phaethon but leave behind solids that can be shed as entrained dust in the sublimative gas outflow, producing the Geminid meteor stream material detected at Earth.

Discussion & Implications. Our sublimative Fe/Pyroxene mass loss model can be tested in Phaethon-like objects by (1) determining the time of onset of outgassing activity; (2) searching for Fe gas in a coma surrounding the object, and then closer in O and SiO, the products of destructive sublimation of pyroxene rock; and (3) determining the surface reflectance spectrum to be consistent with a mix of CAIs + FeOx + olivine + inorganic amorphous/graphitic carbon.

Since we predict total gas production rates of ~10^{22} molecules/s Fe and 10^{21} molecules/s of SiO and O for a few days around each perihelion passage (Fig. 3), observers can use our estimates to predict when any sensible Fe/Si/O comae might be detected. This will help planning for future observations & *in situ* missions.

References. **[1]** Lisse & Steckloff 2022, *Icarus* **381**, 114995 **[2]** Kawakatsu & Itawa 2013 *Adv. Astronaut. Sci.* **146**, 13 **[3]** Arai+ 2018, *LPSC Abstracts* **49**, 2570 **[4]** Jewitt & Hsieh 2006, Astron. J. 132, 1624 **[5]** Hanus et al. 2016, A&A 592, A34 **[6]** Jewitt & Li 2010, Astron. J. 140, 1519 **[7]** Jewitt et al. 2013, Astron. J. 771, L36 **[8]** Jewitt et al. 2018, Astron. J. 156, 238 **[9]** MacLennan et al. 2021, Icarus 366, 114535 **[10]** Green & Davies 1983, IAUC 3878 **[11]** Green et al. 1985, MNRAS 214, 29P **[12]** Tholen 1984, PhD thesis, Univ of Arizona, Tucson **[13]** Kartashova et al. 2019, Contrib. Astron. Obs. Skalnaté Pleso 49, 367 **[14]** Kareta et al. 2018, Astron J 156, 287 **[15]** Jewitt et al. 2019, Astron. J. 157, 193 **[16]** Li & Jewitt 2013, Astron. J. 145, 154 **[17]** Tabeshian et al. 2019, Astron J 158, 30 **[18]** Nagano & Hirabayashi 2020, Astrophys J Lett 892, L22 **[19]** Takir et al. 2020, Nat. Comm. 11, 2050 **[20]** Masiero et al. 2021, Planet. Sci. J. 2, 165 **[21]** Ye et al. 2021, PSJ 2, 23 **[22]** Blaauw 2017, Planetary and Space Science 143, 83 **[23]** Clark et al. 2013, JGR 115, E06005 **[24]** Licandro et al. 2007, A&A 461, 751 **[25]** DeMeo et al. 2009, Icarus 202, 160 **[26]** Kareta et al. 2021, Planet Sci J 2, 190 **[27]** Hiroi et al. 1996, Meteorit. Planet. Sci., 31, 321 **[28]** Hiroi et al. 2004, LPSC Abstracts 35, 1616 **[29]** Vervack et al. 2021, Bulletin of the AAS 53, 7 **[30]** Springmann et al. 2019, Icarus 324, 104 **[31]** Steckloff et al. 2015, Icarus 258, 430 **[32]** Steckloff et al. 2020, Exoplanets III Poster Presentation **[33]** Steckloff et al. 2021a, Astrophys J. Lett 913, L31 **[34]** Langmuir, 1913, Phys. Rev. 2, 329 **[35]** Tabeshian et al. 2019, Astron J 158, 30 **[36]** Steckloff et al. 2021b, Icarus 356, 113998 **[37]** Lisse et al. 2021, Icarus 356, 114072 **[38]** Domingue et al. 2014, Space Science Reviews 181, 121 **[39]** Kohout et al. 2014, Icarus 237, 75 **[40]** Kohout et al. 2016, 47th LPSC #2042 **[41]** Pieters & Noble 2016, J. Geophys. Res. Planets 121, 1865 **[42]** Quadery et al. 2015, J. Geophys. Res. Planets 120, 643 **[43]** Schelling et al. 2015, in Space Weathering of Airless Bodies, 2052